Influence of absorption and scattering on the velocity of acoustic streaming

Wojciech SECOMSKI, Janusz WÓJCIK, Ziemowit KLIMONDA,
Robert OLSZEWSKI, Andrzej NOWICKI

Department of Ultrasound, Institute of Fundamental Technological Research
Polish Academy of Sciences
Pawińskiego 5B, 02-106 Warszawa, Poland
Wojciech.Secomski@ippt.pan.pl

Streaming velocity depends on intensity and absorption of ultrasound in the media. In some cases, such as ultrasound scattered on blood cells at high frequencies, or the presence of ultrasound contrast agents, scattering affects the streaming speed.
The velocities of acoustic streaming in a blood-mimicking starch suspension in water and Bracco BR14 contrast agent were measured. The source of the streaming was a plane 20MHz ultrasonic transducer. Velocity was estimated from the averaged Doppler spectrum. The single particle driving force was calculated as the integral of the momentum density tensor components. For different starch concentrations, the streaming velocity increased from 8.9 to 12.5mm/s. This corresponds to a constant 14% velocity increase for a 1 g/l increase in starch concentration. For BR14, the streaming velocity remained constant at 7.2mm/s and was independent of the microbubbles concentration. The velocity was less than in reference, within 0.5mm/s measurement error.
Theoretical calculations showed a 16% increase in streaming velocity for 1 g/l starch concentration rise, very similar to the experimental results. The theory has also shown the ability to reduce the streaming velocity by low-density scatterers, as was experimentally proved using the BR14 contrast agent.

Keywords: ultrasound, radiation force, starch, contrast agent, blood, thrombolysis

1. Introduction

The aim of this work was to use the streaming phenomena to assist clot dissolution in blood vessels. Such treatment is called sonothrombolysis. Acoustic streaming is a steady flow in a fluid driven by the acoustic wave propagating in a

lossy medium. Streaming depends on the intensity and absorption of ultrasound in the media.

The radiation pressure gradient causes the acoustic radiation force F [1]:

$$F = \frac{2\alpha I_{TA}}{c} \tag{1}$$

where α is the absorption coefficient, I_{TA} is a time averaged intensity in a given space point and c is the wave propagation velocity in the medium.

Tjotta [2] introduced a simple formula in which the streaming velocity v was proportional to the absorption coefficient α, the beam width $2a$ and the acoustic intensity I_{TA} as well as inversely proportional to the medium viscosity μ and the sound velocity in the medium c:

$$v = \frac{8\alpha I_{TA} a^2}{\mu c} \tag{2}$$

In the above formulas, both radiation force and streaming velocity depend only on the absorption coefficient. For biological tissues, the attenuation coefficient α_{att} is the sum of the absorption coefficient α_A and the scattering coefficient α_S:

$$\alpha_{att} = \alpha_A + \alpha_S \tag{3}$$

Usually, the coefficient αA >> αS and αS may be omitted. In some cases, such as ultrasound scattered on blood cells at frequencies ≥ 20 MHz, or the presence of ultrasound contrast agents, scattering affects the streaming speed. Parallel to measurements, the streaming theoretical description will be modified by introducing the scattering coefficient to equations describing the radiation force and the streaming velocity.

2. Materials and Methods

A single 20 MHz, 2 mm diameter, flat ultrasonic transducer was used to generate the streaming and simultaneous streaming velocity measurements. The transducer was connected to an ultrasonic Doppler flow meter and radiated ultrasound with average acoustic power $P_A = 1.9$ mW and space and time averaged intensity $I_{SATA} = 60$ mW/cm^2. The acoustic medium was distilled water with a suspension of starch or ultrasound contrast microbubbles. The streaming velocity was recorded in a sample volume at a distance of 4mm from the transducer. The direction of the streaming corresponded to the direction of the acoustic wave propagation (Fig.1).

The flow velocity was calculated from the Doppler formula [3]:

$$f_d = f_n \frac{v}{c} 2\cos\theta \tag{4}$$

where f_d is the Doppler shift frequency, f_n is the ultrasound frequency (here, 20 MHz), v is the streaming velocity, c is the speed of sound (here, 1500 m/s) and θ is the angle

between the flow direction and the propagation direction of the ultrasonic wave (here, 0).

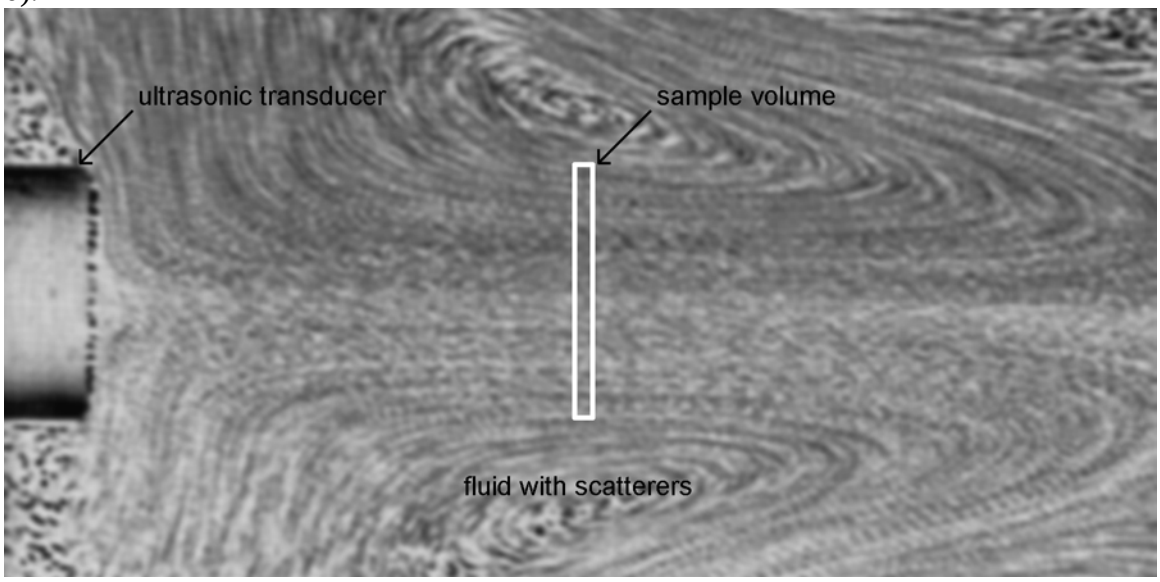

Fig. 1. Experimental setup for streaming generation and simultaneous streaming velocity measurements.

The simplest ultrasonic flow meter is the CW Doppler, whose block diagram is shown in Fig.2 [3]. The ultrasonic transducer is divided into two halves, one transmitting a continuous ultrasonic wave (CW) and the other receiving a signal scattered on the moving particles. The received signal is mixed with the transmitted one. At the output, after low-pass filtering, we get a differential frequency called Doppler shift.

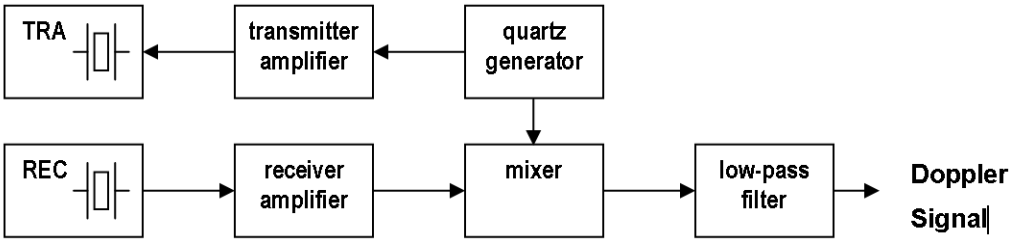

Fig. 2. Block diagram of the CW Doppler flowmeter. TRA - transmitting transducer, REC - receiving transducer.

The received Doppler spectrum from CW Doppler flowmeter is presented in Fig.3. It was assumed that all the particles move at one velocity. The spectrum consists of two lines: the frequency f_n and the Doppler shifted frequency $f_n + f_d$, where f_d is the Doppler shift calculated from equation 4 (Fig.3a). Because the scattering of ultrasonic waves on many particles is random, so instead of a single line we have a spectrum of the stochastic process with the mean frequency $f_n + f_d$ and Gaussian envelope (Fig.3b). After the detection and low-pass filtering, the f_n line is shifted to zero and rejected, so we get a low frequency Doppler spectrum f_d (Fig.3c).

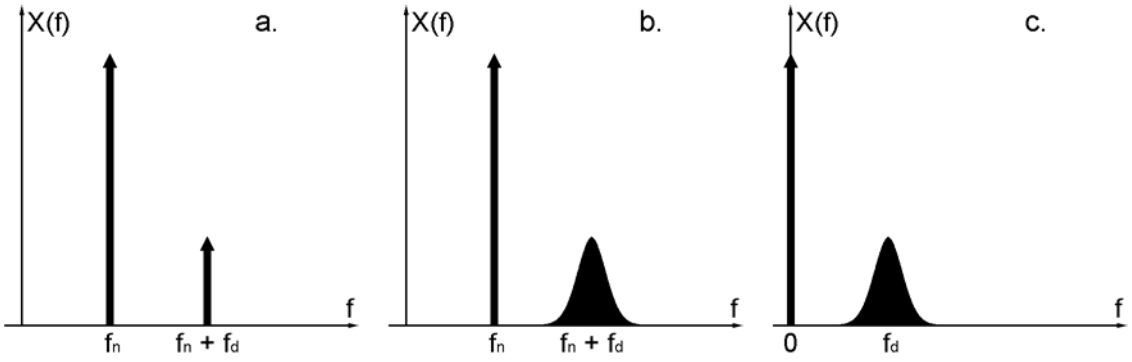

Fig. 3. Signal spectra from CW Doppler flowmeter (not in scale). a. Two-line spectrum for constant flow velocity. b. The real spectrum taking into account the random nature of the scattering on the particles. c. Doppler spectrum after detection and low-pass filtering.

The pulse flowmeter was used in the experiment, where a single ultrasonic transducer alternately transmits f_n frequency bursts and receives a Doppler signal scattered on particles (Fig.4). The received signal is gated and sampled with a fixed delay to the transmitted pulses, and then low-pass filtered. The transmitted pulses are repeated with pulse repetition frequency PRF, and the sampling delay determines the sample volume distances from the ultrasonic transducer.

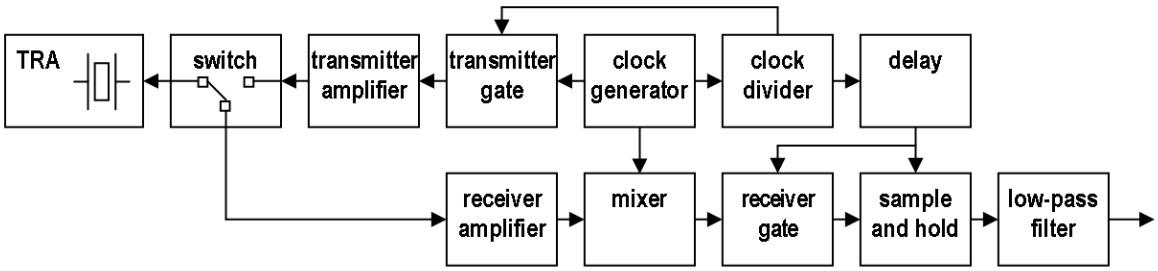

Fig. 4. Block diagram of the pulse Doppler flowmeter. TRA - transmitting and receiving transducer.

The received Doppler spectrum from pulse Doppler flowmeter is presented in Fig.5. It was assumed that all the particles move at one velocity. The transmitted f_n burst spectrum consists of multiple lines separated by PRF frequency: f_n-PRF, f_n, f_n+PRF etc. [4]. To each transmitted line a Doppler signal band is assigned: f_n+f_d-PRF, f_n+f_d, f_n+f_d+PRF etc. (Fig.5a). After detection, sampling-and-holding and low-pass filtering, the f_n lines are shifted to zero and rejected, so we get a low frequency Doppler spectrum f_d (Fig.5b), similar to the CW Doppler flowmeter spectrum.

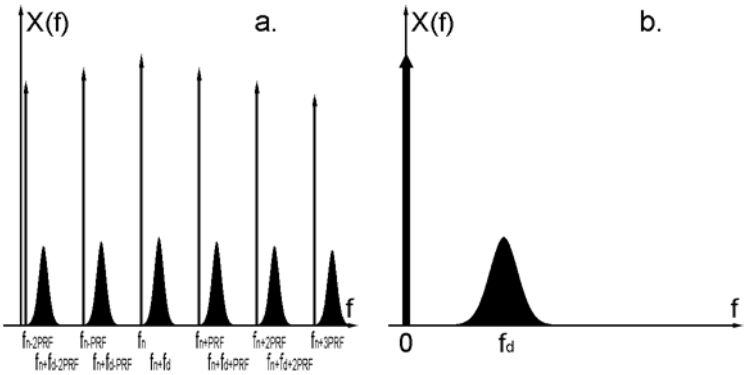

Fig. 5. Signal spectra from pulse Doppler flowmeter (not in scale). a. Multiple-line spectrum for constant flow velocity. b. Doppler spectrum after detection, sampling-and-holding and low-pass filtering.

For the laminar flow, with a parabolic profile, when the ultrasonic beam covers the entire flow, then we obtain a rectangular Doppler spectrum with a constant amplitude from zero to f_{max} (Fig.6a) [3,5]. Under real conditions, for the flow with a flattened profile or when the ultrasonic beam does not cover the entire flow, then we obtain the Doppler spectrum with the highest amplitude at the maximum flow velocity (Fig.6b). Likewise, when measuring the streaming velocity, we expect the spectrum of Fig.6b.

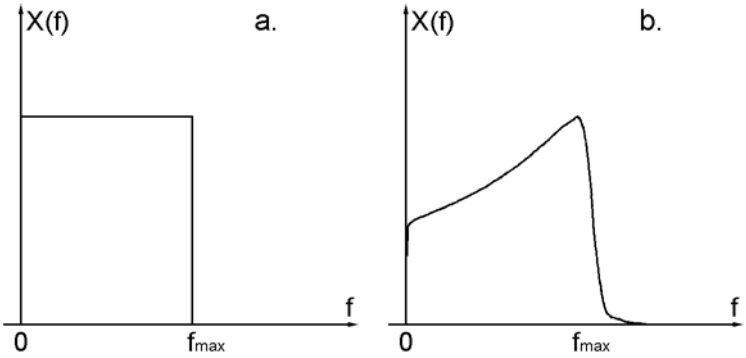

Fig. 6. a. Rectangular Doppler spectrum of the laminar flow, with a parabolic profile, when the ultrasonic beam covers the entire flow. b. Doppler spectrum of the non-laminar flow or when the ultrasonic beam does not cover the entire flow.

The streaming was measured in an aqueous suspension of corn starch. The suspension has blood-like acoustic properties and is used as a blood-mimicking fluid [6]. The suspensions of 1 g/l, 2 g/l, 3 g/l and 4 g/l ($2 \cdot 10^6$ - $8 \cdot 10^6$ particles/mm^3) were investigated. As a reference liquid, a 0.01 g/l aqueous suspension of starch was used. With such a low starch concentration, it was expected that the measured flow velocity would be similar to that of pure water. Concentration of 0.01 g/l was sufficient to obtain 20 dB Doppler amplitude and to estimate the maximum flow velocity. The average diameter of the starch particles was $d_{mean} = 4$ μm, density $\rho = 1.5$ g/cm^3, and the sound velocity in the starch was $c = 2800$ m/s. In the next experiment, the streaming velocity in the microbubble suspension of the Bracco BR14 ultrasonic contrast was measured. Concentrations of $1 \cdot 10^3$, $2 \cdot 10^3$, and $4 \cdot 10^3$ microbubbles/mm^3 were studied. The average diameter of the microbubble was $d_{mean} = 3$ μm. The

Doppler signal from the output of the pulse flowmeter was recorded by the LeCroy 62Xi digital oscilloscope. 50k signal samples were recorded in 1 s. Bandwidth was limited to 0 1.45 kHz at -3db. A 32768 point FFT signal was calculated. The Hamming window was used. Doppler spectrum in 0 - 25 kHz frequency range and $\Delta f = 1.5$ Hz resolution was obtained. Next 50 spectra were averaged. For the reference signal 0.01 g/l starch suspension, 1000 spectra were averaged to obtain a 20 dB noise separation. Finally, the maximum Doppler frequency and the maximum streaming velocity were calculated.

3. Results

The spectra of the Doppler signal for the different concentrations of the corn starch suspension are shown in Fig.7. Spectra for the Bracco BR14 ultrasonic contrast are shown in Fig.8. The calculated maximum streaming speeds for the measured spectra are presented in Table 1. The measured attenuation coefficients of the 20 MHz ultrasound wave in water and in 4 g/l of starch suspension were 0.87 db/cm and 0.93 dB/cm respectively. The streaming velocities calculated from the Tjotta formula (Eq.2) for the above attenuation coefficients are also shown in the table.

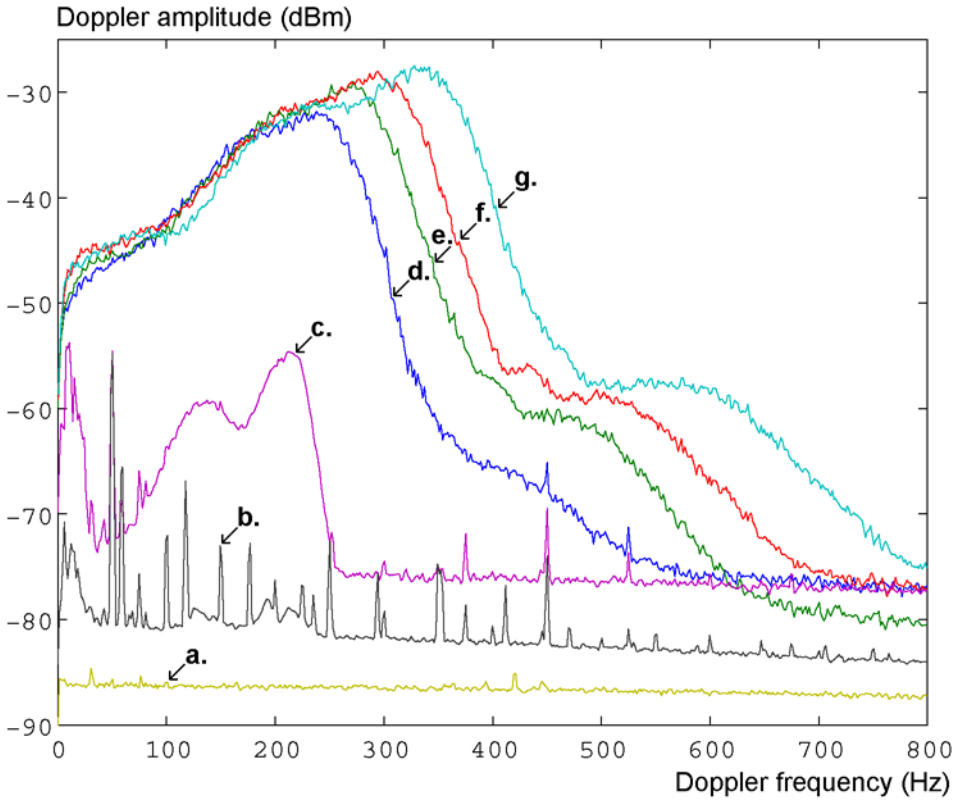

Fig. 7. Spectra of the Doppler signal for the different concentrations of corn starch suspension in water. a. LeCroy 62Xi oscilloscope noise. b. Pulse Doppler flowmeter noise with transducer immersed into distilled water. c. Reference fluid 0.01 g/l starch suspension Doppler spectrum. d. 1 g/l starch suspension. e. 2 g/l starch suspension. f. 3 g/l starch suspension. g. 4 g/l starch suspension. The vertical scale is logarithmic.

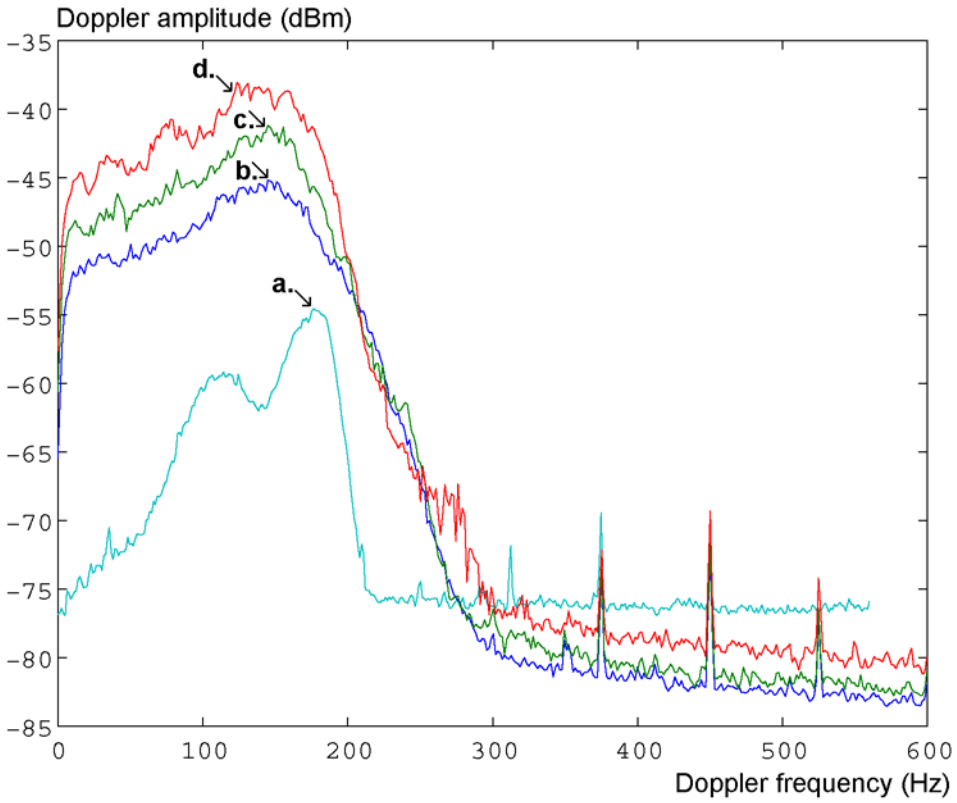

Fig. 8. Spectra of the Doppler signal for the different concentrations of the Bracco BR14 contrast microbubbles suspension in water. a. Reference fluid 0.01 g/l starch suspension Doppler spectrum. b. BR14 contrast agent at $1 \cdot 10^3$ bubbles/mm^3. c. BR14 contrast agent at $2 \cdot 10^3$ bubbles/mm^3. d. BR14 contrast agent at $4 \cdot 10^3$ bubbles/mm^3. The vertical scale is logarithmic.

Tab.1. Maximum streaming velocities calculated from the Tjotta equation and measured in the corn starch and Bracco BR14 contrast suspensions. The percentage change in velocity relative to pure water is shown in the right column.

Tjotta equation H_2O $\alpha = 0.87$ dB/cm	**8.0** mm/s	0
Tjotta equation starch 4 g/l $\alpha = 0.93$ dB/cm	**8.6** mm/s	+ 6.8%
reference 0.01 g/l	**7.9** mm/s ± 0.5 mm/s	- 1.2%
corn starch $2 \cdot 10^6$ particles/mm^3 (1 g/l)	**8.9** mm/s ± 0.5 mm/s	+ 13%
corn starch $4 \cdot 10^6$ particles/mm^3 (2 g/l)	**10.1** mm/s ± 0.5 mm/s	+ 2·14%
corn starch $6 \cdot 10^6$ particles/mm^3 (3 g/l)	**11.0** mm/s ± 0.5 mm/s	+ 3·13%
corn starch $8 \cdot 10^6$ particles/mm^3 (4 g/l)	**12.5** mm/s ± 0.5 mm/s	+ 4·15%
BR14 contrast agent $1 \cdot 10^3$ bubbles/mm^3	**7.2** mm/s ± 0.5 mm/s	- 10%
BR14 contrast agent $2 \cdot 10^3$ bubbles/mm^3	**7.2** mm/s ± 0.5 mm/s	- 10%
BR14 contrast agent $4 \cdot 10^3$ bubbles/mm^3	**7.2** mm/s ± 0.5 mm/s	- 10%

Theoretical considerations:

1. The direction of the radiation force depends on the relationship between the material constants of the inclusions and the surrounding fluid.
2. The streaming velocity may have decreased when the inclusion density was significantly less than the density of the surrounding fluid.
3. The radiation force acting on a single starch particle was $F_a = 7.05 \cdot 10^{-13}$N and the radiation force acting on 1mm^3 of water due to the absorption was $F_w = 8.93 \cdot 10^{-8}$N. The relative increase of the radiation force acting on the starch suspension was equal to $\delta F = q \cdot n_o \cdot F_a \cdot (1mm_3)/F_w =$ **0.158***q (q-times n_o) ($n_o = 2 \cdot 10^6$ particles/mm^3)

4. Conclusions

The maximum streaming velocity in reference fluid was 7.9 mm/s, close to the 8.0 mm/s calculated from the Tjotta equation. For different starch concentrations, the streaming velocity was increasing from 8.9 to 12.5 mm/s. This corresponds to a constant 13% velocity increase for a 1 g/l increase in starch concentration. For BR14, the streaming velocity remained constant at 7.2 mm/s and was independent of the microbubbles concentration. The velocity was less than in reference, within 0.5 mm/s measurement error.

Theoretical calculations showed a 16% increase in streaming velocity for 1g/l starch concentration rise, very similar to the experimental results. The theory has also shown the ability to reduce the streaming velocity by low-density scatterers, as was experimentally proved using the BR14 contrast agent.

Acknowledgments

This investigation was supported by NCN grant 2014/15/B/ST8/04345.

References

[1] W.L. Nyborg, Acoustic streaming, in W.P. Mason, ed., Physical acoustics, IIB, Academic Press, 265-331, New York 1965.
[2] S. Tjotta S, On some non-linear effects in sound fields with special emphasis on generation of vorticity and the formation of streaming patterns, Arch.Math. Naturvidensk., 55, 1-68, 1959.
[3] L. Filipczynski, R. Herczynski, A. Nowicki, T. Powalowski, Przepływ krwi, 67-102, Państwowe Wydawnictwo Naukowe, Warszawa 1980.
[4] J. Szabatin, Podstawy teorii sygnałów, Wydawnictwa Komunikacji i Łączności, 245-346, Warszawa 2000.
[5] S. Ricci, R. Matera, P. Tortoli, An improved Doppler model for obtaining accurate maximum blood velocities, Ultrasonics 54 (7): 2006–2014, 2014.
[6] T. Yoshida, K. Tanaka, K. Sato, T. Kondo, K. Yasukawa, N. Miyamoto, M. Taniguchi, Blood-Mimicking Fluid for the Doppler Test Objects of Medical Diagnostic Instruments, 2012 IEEE International Ultrasonics Symposium, DOI: 10.1109/ULTSYM.2012.0403, 1-4, 2012.